Phytopathologia Mediterranea
The international journal of the
Mediterranean Phytopathological Union

Firenze University Press
www.fupress.com/pm

Research Papers

Neocosmospora spp. associated with dry root rot of citrus in South Africa

Vladimiro GUARNACCIA[1,2,3,*], Jan VAN NIEKERK[3,4], Pedro W. CROUS[5], Marcelo SANDOVAL-DENIS[5]

[1] *Centre for Innovation in the Agro-Environmental Sector, AGROINNOVA, University of Torino, Largo Braccini 2, 10095 Grugliasco (TO), Italy*
[2] *Department of Agricultural, Forest and Food Sciences (DISAFA), University of Torino, Largo Braccini 2, 10095 Grugliasco (TO), Italy*
[3] *Department of Plant Pathology, University of Stellenbosch, Private Bag X1, Matieland 7602, South Africa*
[4] *Citrus Research International, P.O. Box 28, Nelspruit 1200, South Africa*
[5] *Westerdijk Fungal Biodiversity Institute Uppsalalaan 8, 3584 CT, Utrecht, The Netherlands*
*Corresponding author. E-mail: vladimiro.guarnaccia@unito.it

Summary. Citrus is one of the most important fruit crops cultivated in South Africa. Internationally, citrus dry root rot is a common disease in major citrus production areas. Several abiotic and biotic factors are involved in disease development, in which *Neocosmospora* species are important biotic agents. The diversity of *Neocosmospora* species associated with dry root rot symptoms of *Citrus* trees cultivated in South Africa was evaluated using morphological and molecular analyses. Multi-locus analysis was conducted, based on fragments of seven loci including: ATP citrate lyase (*acl1*), calmodulin (*cal*), internal transcribed spacer region of the rRNA (ITS), large subunit of the rRNA (LSU), RNA polymerase largest subunit (*rpb1*), RNA polymerase second largest subunit (*rpb2*), and translation elongation factor 1-alpha (*tef1*). A total of 62 strains representing 11 *Neocosmospora* species were isolated from crowns, trunks and roots of citrus trees affected by dry root rot, as well as from soils sampled in affected citrus orchards. The most commonly isolated taxa were *N. citricola*, *N. ferruginea* and *N. solani*, while rarely encountered taxa included *N. brevis*, *N. crassa*, *N. hypothenemi* and *N. noneumartii*. Furthermore, four *Neocosmospora* species are also newly described, namely *N. addoensis*, *N. citricola*, *N. gamtoosensis* and *N. lerouxii*.

Keywords. Citrus decline, morphology, multigene phylogeny, systematics.

OPEN ACCESS

Citation: V. Guarnaccia, J. van Niekerk, P. W. Crous, M. Sandoval-Denis (2021) *Neocosmospora* spp. associated with dry root rot of citrus in South Africa. *Phytopathologia Mediterranea* 60(1): 79-100. doi: 10.36253/phyto-12183

Accepted: January 24, 2021

Published: May 15, 2021

Data Availability Statement: All relevant data are within the paper and its Supporting Information files.

Competing Interests: The Author(s) declare(s) no conflict of interest.

Editor: Alan J.L. Phillips, University of Lisbon, Portugal.

INTRODUCTION

Citrus is one of the most important world fruit crops, and South Africa is among the largest producers and exporters of citrus fruit (FAOSTAT, 2019). Citrus dry root rot (DRR) is a common problem among citrus growers, reported in major production areas such as Australia (Broadbent, 2000), Florida, California and Texas in the United States of America (Graham *et*

al., 1985), Italy (Polizzi *et al*., 1992), Oman (Nemec *et al*., 1980; Bender, 1985), Pakistan (Kore and Mane, 1992; Conzulex *et al*., 1997; Verma *et al*., 1999; Rehman *et al*., 2012), Turkey (Kurt *et al*., 2020), Tunisia, Greece and Egypt (El-Mohamedy, 1998; Yaseen and D'Onghia, 2012).

While the aetiology of DRR is multifactorial and not completely understood, it is usually attributed to *Neocosmospora* (*Fusarium*) *solani* sensu lato. However, several species of *Neocosmospora*, but also *Fusarium*, are commonly found in orchard soils and citrus plants. These two closely related fusarioid genera encompass important plant pathogens, and are associated with major diseases of citrus (Menge, 1988; Derrick and Timmer, 2000; Sandoval-Denis *et al*., 2018), including DRR, root rot, feeder root rot, wilt, twig dieback and citrus decline (Menge, 1988; Spina *et al*., 2008). *Fusarium equiseti* was recovered from citrus roots in Florida (Smith *et al*., 1988), while *F. proliferatum*, *F. sambucinum* and *Neocosmospora solani* were found in Greece (Malikoutsaki-Mathioudi *et al*., 1987). *Fusarium oxysporum* f. sp. *citri* was reported as responsible for the wilt of citrus in Tunisia (Hannachi *et al*., 2014). *Fusarium oxysporum* and strains first assigned to "*F. ensiforme*" and later reidentified as *Neocosmospora brevis* were also reported from DRR in Italy (Sandoval-Denis *et al*., 2018; 2019), while a number of *Neocosmospora* species have been reported in association with DRR of citrus in Europe (Sandoval-Denis *et al*., 2018).

Neocosmospora (*Hypocreales*, *Nectriaceae*), comprises species with varied ecologies, including saprobes, endophytes, and plant and animal pathogens. Pathogenic species of *Neocosmospora* are known to affect more than 100 plant host families and diverse animal species, including humans (Sandoval-Denis *et al*., 2019). Although *Neocosmospora* (1899) is an old and well-established name, recent phylogenetic, morphological and ecological data (Lombard *et al*., 2015) provided additional support for this genus as one of several distinct fusarioid genera in the *Nectriaceae*. Follow-up revisions have corrected the taxonomy of most *Neocosmospora* species known to date, including the main pathogenic clades (Sandoval-Denis and Crous, 2018; Sandoval-Denis *et al*., 2019).

Previous studies have demonstrated how DRR, caused by the association between stressed plants and *Neocosmospora* species, can generate sudden decline of plants weakened by abiotic and biotic factors, such as root injuries, Phytophthora root rot, graft incompatibility, poor drainage, poor soil aeration, excess fertilizer, or soil pH (Menge, 1988; Polizzi *et al*., 1992). Chlorosis, poor vigour, wilt, leaf abscission and degeneration are visible in affected plants for several years before they suddenly die. Examination of scaffold roots, crowns and basal trunks usually shows wood staining (Timmer *et al*., 1979; Timmer 1982). Rot of the fibrous roots is also visible and associated with canopy size reductions, defoliation, dieback and sloughing of root cortices (Nemec and Baker, 1992). This disease has been managed by planting resistant rootstocks. However, during the last decade, trifoliate orange (*Poncirus trifoliata*) rootstocks, which are very susceptible to DRR, have been widely used, due to their resistance to virus and soilborne pathogens (i.e.: Citrus Tristeza Virus) (Fang *et al*., 1998).

Since 2013, sudden, devastating decline and death of citrus trees has been reported in the Gamtoos and Sundays River Valleys production areas in the Eastern Cape province of South Africa. This decline is typically observed on 4– to 10-year-old trees with the trifoliate rootstocks Carrizo citrange and Swingle citrumelo. As scions, these declining trees are of various citrus types, including lemons, oranges and mandarins. To date, little is known about DRR-like diseases in citrus orchards in South Africa. Given the importance of citrus production, and specifically in the two areas of South Africa, as well as the relevant economic impact of DRR in other countries, further research was needed to increase understanding of the aetiology of this disease.

Morphological, cultural and molecular characteristics of the fungal species associated with symptomatic trees were investigated in this study by employing large-scale sampling to isolate the pathogens involved, and to identify their strains according to modern taxonomic concepts *via* morphological characterization and multi-locus DNA sequence data. In 2018 several surveys were conducted in citrus orchards with the aims to: (1) conduct extensive surveys to sample symptomatic plant material; (2) cultivate as many of the associated fungi as possible; (3) conduct DNA multi-locus sequence analyses combined with morphological characterization of isolates obtained; and (4) compare the obtained results with known wood decay fungi previously associated with trees displaying characteristic DDR symptoms.

MATERIALS AND METHODS

Sampling, fungal collection and isolation

The Patensie (Gamtoos River Valley) and Kirkwood (Sundays River Valley) areas were surveyed during the second half of 2018. During these visits, the external and internal symptoms of diseased trees were examined. Scaffold roots, crown and trunk portions taken from between soil level and scion unions, were collected in

both the survey areas. Samples were each transversally cut into 3-cm-thick discs, which allowed observation of internal wood decay symptoms.

Wood fragments (3 × 3 mm) were cut from necrotic and healthy tissues and also from the margins between them. Each fragment was then surface sterilised by soaking in 70% ethanol for 5 s, 4% sodium hypochlorite for 90 s, sterile water for 60 s and then dried on sterile filter paper. Fragments were placed on potato dextrose agar (PDA) amended with 100 µg mL^{-1} streptomycin (PDA-S), and were then incubated at 25°C. Characteristic *Neocosmospora* colonies were collected from these plates by hyphal tipping onto clean PDA-S plates. The isolates used in this study are maintained in the culture collection of the Department of Plant Pathology, University of Stellenbosch, Stellenbosch, South Africa, and at the Westerdijk Fungal Biodiversity Institute (CBS), Utrecht, The Netherlands (Table 1).

Morphological studies of isolates

Morphological studies were carried out as indicated elsewhere (Leslie and Summerell, 2006; Sandoval-Denis and Crous, 2018; Sandoval-Denis *et al*., 2019). Macroscopic characteristics and fungal colony appearance of each isolate was determined after culturing on oatmeal agar (OA), potato dextrose agar (PDA) and synthetic nutrient-poor agar (SNA; Nirenberg, 1976), and incubation for 7–14 d at 24°C in darkness under a 12 h/12 h light/darkness cycle using cool fluorescent light. Colour nomenclature follows that of Rayner (1970). Fungal micromorphology was studied using 7–14-d-old cultures on carnation leaf agar (CLA; Fisher *et al*., 1982) and SNA, incubated at 24°C in a 12 h/12 h near UV light/dark cycle. Photomicrographs were captured using a Nikon Eclipse 80i microscope with Differential Interference Contrast (DIC) optics and a Nikon AZ100 dissection microscope, both equipped with a Nikon DS-Ri2 high definition colour digital camera. Measurements were recorded using Nikon NIS-elements D software v. 4.50, from at least 50 randomly selected elements for each structure.

Molecular studies of isolates

Total genomic DNA was extracted from isolates grown on malt extract agar (MEA; Crous *et al*., 2019), incubated for 7 d at room temperature (approx. 24°C). Mycelium was scraped from the colony surfaces with the aid of sterile scalpels, and DNA was isolated using the Wizard® Genomic DNA purification Kit (Promega Corporation) following the manufacturer's protocol.

Seven gene fragments were PCR amplified using the following primer combinations with protocols described elsewhere: acl1-230up and acl1-1220low for the larger subunit of the ATP citrate lyase (*acl1*; Gräfenhan *et al*. 2011), CAL-228F and CAL2Rd for calmodulin (*cal*; Carbone and Kohn, 1999; Quaedvlieg *et al*., 2014), ITS4 and ITS5 for the internal transcribed spacer region of the rRNA (ITS; White *et al*., 1990), LR0R and LR5 for a partial fragment of the large subunit of the rRNA (LSU; Vilgalys and Hester, 1990; Vilgalys and Sun, 1994), Fa and G2R for the RNA polymerase largest subunit (*rpb1*; O'Donnell *et al*., 2010), 5f2 and 7cr plus 7cf and 11ar for two non-contiguous fragments of the RNA polymerase second largest subunit (*rpb2*: Liu *et al*., 1999; Sung *et al*. 2007), and EF-1 and EF-2 for the translation elongation factor 1-alpha gene (*tef1*: O'Donnell *et al*., 2008). Sequencing was carried out in both directions on an ABI Prism 3730XL DNA Analyzer (Applied Biosystems) using the same primer pairs used for amplification, plus the internal sequencing primers F6, F8 and R8 for *rpb1* (O'Donnell *et al*., 2010). Consensus sequences were assembled using Seqman Pro v. 10.0.1 (DNASTAR).

Sequence alignments were constructed and analysed individually for each gene partition, including DNA sequences representing the phylogenetic diversity of *Neocosmospora* selected according to recently published phylogenies (Guarnaccia *et al*., 2019; Sandoval-Denis *et al*., 2019). Alignments were achieved using MAFFT (Katoh *et al*., 2019) as implemented on the European Bioinformatics Institute (EMBL-EBI) portal (www.ebi.ac.uk), and were visually inspected and then manually corrected if needed using MEGA v. 6 (Tamura *et al*., 2013).

Phylogenetic analyses were based on two independent algorithms: Maximum-Likelihood, using Random Accelerated (*sic*) Maximum Likelihood (RAxML) v. 8.2.10 (Stamatakis, 2014) and Bayesian inference (BI) under MrBayes v. 3.2.6 (Huelsenbeck and Ronquist, 2001; Ronquist and Huelsenbeck, 2003). The analyses were carried out using the CIPRES Science Gateway portal (www.phylo.org: Miller *et al*., 2012). Single-gene phylogenies were compared visually to check for topological conflict between significantly supported clades, and then as combined multilocus phylogenies (Mason-Gamer and Kellogg, 1996; Wiens 1998). A first analysis based on combined *rpb2* and *tef1* sequence data was directed to identify *Neocosmospora* spp. from isolates obtained from symptomatic citrus trees. A second analysis including the combined seven gene dataset was directed to clarify the phylogeny of South African citrus *Neocosmospora* isolates with uncertain phylogenetic position or deter-

Table 1. Collection data and GenBank accession numbers of isolates included in this study.

Species	Strain number[1]	Country	Host	GenBank sequence accession number[2]						
				acl	*cal*	ITS	LSU	*rpb1*	*rpb2*	*tef1*
Geejayessia atrofusca	NRRL 22316	USA	Staphylea trifolia	-	-	AF178423	AF178392	JX171496	EU329502	AF178361
Geejayessia cicatricum	CBS 125552	Slovenia	Dead twig	HQ728171	-	HQ728145	MH875038	-	HQ728153	HM626644
Neocosmospora addoensis	CBS 146508 = VG268 = CPC 37126	South Africa	*Citrus sinensis* - crown	MW218003	MW218050	MW173040	MW173031	MW218096	MW446573	MW248739
	CBS 146509 = VG279 = CPC 37127	South Africa	*Citrus sinensis* - crown	MW218004	MW218051	MW173041	MW173032	MW218097	MW446574	MW248740
	CBS 146510^{T} = VG281 = CPC 37128	South Africa	*Citrus sinensis* - crown	MW218005	MW218052	MW173042	MW173033	MW218098	MW446575	MW248741
Neocosmospora ampla	CBS 202.32^{T}	German East Africa	*Coffea* sp.	-	-	LR583701	LR583909	-	LR583815	LR583594
Neocosmospora bataticola	CBS 144397	USA	Ipomoea batatas	MW218006	MW218053	AF178407	AF178376	MW218099	EU329509	AF178343
	CBS 144398^{T}	USA	Ipomoea batatas	MW218007	MW218054	AF178408	AF178377	MW218100	FJ240381	AF178344
Neocosmospora borneensis	CBS 145462^{ET}	Indonesia	Bark or recently dead tree	-	-	AF178415	AF178384	-	EU329515	AF178352
Neocosmospora bostrycoides	CBS 144.25^{NT}	Honduras	Soil	MW218008	MW218055	LR583704	LR583912	MW218101	LR583818	LR583597
	CBS 392.66	Unknown	Bertholletia excelsa	MW218009	MW218056	LR583705	LR583913	MW218102	LR583819	LR583598
Neocosmospora brevicona	CBS 204.31^{ET}	Indonesia	*Gladiolus* sp.	MW218010	MW218057	LR583707	LR583915	MW218103	LR583821	LR583600
Neocosmospora brevis	CBS 130326	USA	Human eye	-	-	DQ094351	DQ236393	-	EF470136	DQ246869
	VG150	South Africa	*Citrus sinensis* - crown	-	-	MW173043	-	-	MW446576	MW248742
	VG152	South Africa	*Citrus sinensis* - crown	-	-	MW173044	-	-	MW446577	MW248743
	VG157	South Africa	*Citrus sinensis* - crown	-	-	MW173045	-	-	MW446578	MW248744
Neocosmospora catenata	CBS 143228	USA	*Stegostoma fasciatum*	MW218011	MW218058	KC808255	KC808255	MW218104	KC808354	KC808213
	CBS 143229^{T}	USA	*Stegostoma fasciatum*	MW218012	MW218059	KC808256	KC808256	MW218105	KC808355	KC808214
Neocosmospora citricola	CBS 146511 = VG302 = CPC 37129	South Africa	*Citrus sinensis* - crown	MW218013	MW218060	MW173046	MW173034	MW218106	MW446579	MW248745
	CBS 146512 = VG307 = CPC 37130	South Africa	*Citrus sinensis* - crown	MW218014	MW218061	MW173047	MW173035	MW218107	MW446580	MW248746
	CBS 146513^{T} = VG343 = CPC 37131	South Africa	*Citrus sinensis* - crown	MW218015	MW218062	MW173048	MW173036	MW218108	MW446581	MW248747
	VG17	South Africa	*Citrus sinensis* - crown	-	-	MW173049	-	-	MW446582	MW248748
	VG30	South Africa	*Citrus sinensis* - crown	-	-	MW173050	-	-	MW446583	MW248749
	VG139	South Africa	*Citrus sinensis* - crown	-	-	MW173051	-	-	MW446584	MW248750
	VG140	South Africa	*Citrus sinensis* - crown	-	-	MW173052	-	-	MW446585	MW248751
	VG183	South Africa	*Citrus sinensis* - crown	-	-	MW173053	-	-	MW446586	MW248752
	VG197	South Africa	*Citrus sinensis* - root scaffold	-	-	MW173054	-	-	MW446587	MW248753
	VG203	South Africa	*Citrus sinensis* - crown	-	-	MW173055	-	-	MW446588	MW248754

(Continued)

Table 1. (Continued).

Species	Strain number[1]	Country	Host	GenBank sequence accession number[2]						
				acl	*cal*	ITS	LSU	*rpb1*	*rpb2*	*tef1*
	VG287	South Africa	*Citrus sinensis* - crown	-	-	MW173056	-	-	MW446589	MW248755
	VG332	South Africa	*Citrus sinensis* - crown	-	-	MW173057	-	-	MW446590	MW248756
	VG358	South Africa	*Citrus sinensis* - crown	-	-	MW173058	-	-	MW446591	MW248757
	VG389	South Africa	*Citrus sinensis* - crown	-	-	MW173059	-	-	MW446592	MW248758
	VG399	South Africa	*Citrus sinensis* - crown	-	-	MW173060	-	-	MW446593	**MW248759**
Neocosmospora crassa	CBS 144386^{T}	France	Unknown	**MW218016**	**MW218063**	LR583709	LR583917	**MW218109**	LR583823	LR583604
	VG211 = CPC 37122	South Africa	*Citrus sinensis* - crown	-	-	**MW173061**	**MW173037**	-	**MW446594**	**MW248760**
Neocosmospora cucurbitae	CBS 410.62	Netherlands	*Cucurbita viciifolia*	-	-	LR583710	LR583918	-	LR583824	DQ247640
	CBS 616.66^{T}	Netherlands	*Cucurbita viciifolia*	-	-	LR583711	LR583919	-	LR583825	DQ247592
Neocosmospora cyanescens	CBS 518.82^{T}	Netherlands	Human foot	**MW218017**	**MW218064**	AB190389	LR583920	**MW218110**	LR583826	LR583605
	CBS 637.82	Netherlands	Human foot	**MW218018**	**MW218065**	LR583712	LR583921	**MW218111**	LR583827	LR583606
Neocosmospora diminuta	CBS 144390^{T}	Unknown	*Coelocaryon preusii*	-	-	LR583713	LR583922	-	LR583828	LR583607
Neocosmospora elegans	CBS 144395	Japan	*Xanthoxylum piperitum*	**MW218019**	**MW218066**	AF178394	AF178363	**MW218112**	EU329496	AF178328
	CBS 144396^{ET}	Japan	*Xanthoxylum piperitum*	**MW218020**	**MW218067**	AF178401	AF178370	**MW218113**	FJ240380	AF178336
Neocosmospora falciformis	CBS 475.67^{T}	Puerto Rico	Human mycetoma	**MW218021**	**MW218068**	MG189935	MG189915	**MW218114**	LT960558	LT906669
	CBS 121450	Syria	Declined grape vine	**MW218022**	**MW218069**	JX435211	JX435211	**MW218115**	JX435261	JX435161
	VG296	South Africa	soil - citrus orchard	-	-	**MW173062**	-	-	**MW446595**	**MW248761**
Neocosmospora ferruginea	CBS 109028^{T}	Switzerland	Human subcutaneous nodule	-	-	DQ094446	DQ236488	-	EU329581	DQ246979
	VG21	South Africa	*Citrus sinensis* - crown			MW440622			MW446596	MW446558
	VG22	South Africa	*Citrus sinensis* - crown			MW440623			MW446597	MW446559
	VG51	South Africa	*Citrus sinensis* - root scaffold			MW440624			MW446598	MW446560
	VG98	South Africa	*Citrus sinensis* - crown			MW440625			MW446599	MW446561
	VG109	South Africa	*Citrus sinensis* - crown			MW440626			MW446600	MW446562
	VG133	South Africa	*Citrus sinensis* - root scaffold			MW440627			MW446601	MW446563
	VG159	South Africa	*Citrus sinensis* - root scaffold			MW440628			MW446602	MW446564
	VG191	South Africa	*Citrus sinensis* - crown			MW440629			MW446603	MW446565
	VG195	South Africa	*Citrus sinensis* - root scaffold			MW440630			MW446604	MW446566
	VG205	South Africa	*Citrus sinensis* - root scaffold			MW440631			MW446605	MW446567

(Continued)

Table 1. (Continued).

Species	Strain number[1]	Country	Host	GenBank sequence accession number[2]						
				acl	*cal*	ITS	LSU	*rpb1*	*rpb2*	*tef1*
	VG289	South Africa	*Citrus sinensis* - root scaffold			MW440632			MW446606	MW446568
	VG370	South Africa	*Citrus sinensis* - crown			MW440633			MW446607	MW446569
	VG371	South Africa	*Citrus sinensis* - crown			MW440634			MW446608	MW446570
	VG394	South Africa	*Citrus sinensis* - root scaffold			MW440635			MW446609	MW446571
	VG403	South Africa	*Citrus sinensis* - crown			MW440636			**MW446610**	**MW446572**
Neocosmospora gamsii	CBS 143207^{T}	USA	Human bronchoalveolar lavage fluid	-	-	DQ094420	DQ236462	-	EU329576	DQ246951
	CBS 143211	USA	Humidifier coolant	-	-	DQ094563	DQ236605	-	EU329622	DQ247103
Neocosmospora gamtoosensis	CBS 146502^{T} = VG16 = CPC 37120	South Africa	*Citrus sinensis - crown*	**MW218023**	**MW218070**	**MW173063**	**MW173038**	**MW218116**	**MW446611**	**MW248762**
Neocosmospora haematococca	CBS 119600^{ET}	Sri Lanka	Dying tree	-	-	KM231797	KM231664	-	LT960561	DQ247510
Neocosmospora hypothenemi	CBS 145464^{T}	Benin	*Hypothenemus hampei*	**MW218024**	-	LR583715	LR583923	**MW218117**	JF741176	JF740850
	CBS 145466	Uganda	*Hypothenemus hampei*	**MW218025**	**MW218071**	-	-	**MW218118**	-	-
	VG11	South Africa	*Citrus sinensis* - crown	-	-	**MW173064**	-	-	**MW446612**	**MW248763**
	VG14	South Africa	*Citrus sinensis* - crown	-	-	**MW173065**	-	-	**MW446613**	**MW248764**
	VG49	South Africa	*Citrus sinensis* - root scaffold	-	-	**MW173066**	-	-	**MW446614**	**MW248765**
	VG189	South Africa	*Citrus sinensis* - crown	-	-	**MW173067**	-	-	**MW446615**	**MW248766**
	VG328	South Africa	*Citrus sinensis* - crown	-	-	**MW173068**	-	-	**MW446616**	**MW248767**
Neocosmospora ipomoeae	CBS 353.87	Netherlands	*Gerbera* sp.	**MW218026**	**MW218072**	LR583717	LR583925	**MW218119**	LR583831	DQ247639
	CBS 833.97	Netherlands	*Rosa* sp.	**MW218027**	**MW218073**	LR583719	LR583927	**MW218120**	LR583833	LR583611
Neocosmospora keratoplastica	CBS 490.63^{T}	Japan	Human	**MW218028**	**MW218074**	LR583721	LR583929	**MW218121**	LT960562	LT906670
	CBS 144389	Belgium	Greenhouse humic soil	**MW218029**	**MW218075**	LR583722	LR583930	**MW218122**	LR583836	LR583613
Neocosmospora lerouxii	CBS 146514^{T} = VG48 = CPC 37132	South Africa	*Citrus sinensis* - root scaffold	**MW218030**	**MW218076**	**MW173069**	**MW173039**	**MW218123**	**MW446617**	**MW248768**
Neocosmospora lichenicola	CBS 509.63	Brazil	Air	-	-	LR583728	LR583936	-	LR583843	LR583618
	CBS 623.92^{ET}	Germany	Human necrotic wound	-	-	LR583730	LR583938	-	LR583845	LR583620
Neocosmospora liriodendri	CBS 117481^{T}	USA	*Liriodendron tulipifera*	**MW218031**	**MW218077**	AF178404	AF178373	**MW218124**	EU329506	AF178340
Neocosmospora longissima	CBS 126407^{T}	New Zealand	Tree bark	-	-	LR583731	LR583939	-	LR583846	LR583621
Neocosmospora macrospora	CBS 142424^{T}	Italy	*Citrus sinensis*	**MW218032**	**MW218078**	LT746266	LT746281	**MW218125**	LT746331	LT746218
	CPC 28193	Italy	*Citrus sinensis*	**MW218033**	**MW218079**	LT746268	LT746283	**MW218126**	LT746333	LT746220

(Continued)

Table 1. (Continued).

Species	Strain number[1]	Country	Host	GenBank sequence accession number[2]						
				acl	*cal*	ITS	LSU	*rpb1*	*rpb2*	*tef1*
Neocosmospora martii	CBS 115659^{ET}	Germany	*Solanum tuberosum*	-	-	JX435206	JX435206	-	JX435256	JX435156
Neocosmospora metavorans	CBS 135789^{T}	Greece	Human pleural effusion	**MW218034**	**MW218080**	LR583738	LR583946	**MW218127**	LR583849	LR583627
	CBS 143219	Spain	Human foot	**MW218035**	**MW218081**	LR583744	LR583948	**MW218128**	LR583851	LR583629
Neocosmospora mori	CBS 145467^{T}	Japan	*Morus alba*	-	-	DQ094305	DQ236347	-	EU329499	AF178358
	CBS 145468	Japan	*Morus alba*	-	-	DQ094306	DQ236348	-	EU329493	AF178359
Neocosmospora noneumartii	CBS 115658^{T}	Israel	*Solanum tuberosum*	**MW218036**	**MW218082**	LR583745	LR583949	**MW218129**	**MW446618**	LR583630
	VG87 = CPC 37135	South Africa	*Citrus sinensis* - root scaffold	-	-	**MW173070**	**MW173345**	-	**MW446619**	**MW248769**
	VG88 = CPC 37136	South Africa	*Citrus sinensis* - root scaffold	-	-	**MW173071**	**MW173346**	-	**MW446620**	**MW248770**
Neocosmospora oblonga	CBS 130325^{T}	USA	Human eye	-	-	LR583746	LR583950	-	LR583853	LR583631
Neocosmospora paraeumartii	CBS 487.76^{T}	Argentina	*Solanum tuberosum*	-	-	LR583747	LR583951	-	LR583855	DQ247549
Neocosmospora parceramosa	CBS 115695^{T}	South Africa	Soil	**MW218037**	**MW218083**	JX435199	JX435199	-	JX435249	JX435149
Neocosmospora perseae	CBS 144142^{T}	Italy	*Persea americana*	**MW218038**	**MW218084**	LT991940	LT991947	**MW218130**	LT991909	LT991902
Neocosmospora petroliphila	CBS 203.32	South Africa	*Pelargonium* sp.	**MW218039**	**MW218085**	DQ094320	DQ236362	**MW218131**	LR583857	DQ246835
	CBS 224.34	Cuba	Human toenail	**MW218040**	**MW218086**	DQ094383	DQ236425	**MW218132**	LR583858	DQ246910
Neocosmospora piperis	CBS 145470^{T}	Brazil	*Piper nigrum*	-	-	AF178422	AF178391	-	EU329513	AF178360
Neocosmospora pisi	CBS 123669^{ET}	USA	Progeny of parentals from *Pisum sativum* and soil	-	-	LR583753	LR583957	-	LR583862	LR583636
	CBS 142372	Germany	*Trifolium subterraneum*	-	-	LR583755	LR583959	-	LR583864	KY556454
Neocosmospora protoensiformis	CBS 145471^{T}	Venezuela	Dicot tree	-	-	AF178399	AF178368	-	EU329498	AF178334
Neocosmospora pseudoradicicola	CBS 145472^{T}	Papua New Guinea	Diseased cocoa pods	**MW218041**	**MW218087**	JF740899	JF740899	**MW218133**	JF741084	JF740757
Neocosmospora quercicola	CBS 141.90^{T}	Italy	*Quercus cerris*	-	-	LR583760	LR583964	-	LR583869	DQ247634
Neocosmospora regularis	CBS 230.34^{T}	Netherlands	*Pisum sativum*	-	-	LR583763	LR583967	-	LR583873	LR583643
Neocosmospora silvicola	CBS 123846^{T}	USA	*Liriodendron tulipifera*	-	-	LR583766	LR583971	-	LR583876	LR583646
Neocosmospora solani	CBS 140079^{ET}	Slovenia	*Solanum tuberosum*	**MW218042**	**MW218088**	KT313633	KT313633	**MW218134**	KT313623	KT313611
	VG36	South Africa	*Citrus sinensis* - root scaffold	-	-	**MW173072**	-	-	**MW446621**	**MW248771**
	VG38	South Africa	*Citrus sinensis* - root scaffold	-	-	**MW173073**	-	-	**MW446622**	**MW248772**

(Continued)

Table 1. (Continued).

Species	Strain number[1]	Country	Host	GenBank sequence accession number[2]						
				acl	*cal*	ITS	LSU	*rpb1*	*rpb2*	*tef1*
	VG46	South Africa	*Citrus sinensis* - root scaffold	-	-	**MW173074**	-	-	**MW446623**	**MW248773**
	VG53	South Africa	*Citrus sinensis* - root scaffold	-	-	**MW173075**	-	-	**MW446624**	**MW248774**
	VG63	South Africa	*Citrus sinensis* - root scaffold	-	-	**MW173076**	-	-	**MW446625**	**MW248775**
	VG68	South Africa	*Citrus sinensis* - root scaffold	-	-	**MW173077**	-	-	**MW446626**	**MW248776**
	VG78	South Africa	*Citrus sinensis* - root scaffold	-	-	**MW173078**	-	-	**MW446627**	**MW248777**
	VG93	South Africa	*Citrus sinensis* - root scaffold	-	-	**MW173079**	-	-	MW446628	MW248778
	VG99	South Africa	Soil - citrus orchard	-	-	**MW173080**	-	-	**MW446629**	**MW248779**
	VG115	South Africa	*Citrus sinensis* - crown	-	-	**MW173081**	-	-	**MW446630**	**MW248780**
	VG147	South Africa	*Citrus sinensis* - crown	-	-	**MW173082**	-	-	**MW446631**	**MW248781**
	VG169	South Africa	*Citrus sinensis* - crown	-	-	**MW173083**	-	-	**MW446632**	**MW248782**
	VG175	South Africa	*Citrus sinensis* - root scaffold	-	-	**MW173084**	-	-	**MW446633**	**MW248783**
	VG193	South Africa	*Citrus sinensis* - root scaffold	-	-	**MW173085**	-	-	**MW446634**	**MW248784**
	VG415	South Africa	*Citrus sinensis* - crown	-	-	**MW173086**	-	-	**MW446635**	**MW248785**
Neocosmospora sp. (FSSC12)	CBS 143212	USA	Turtle egg	**MW218043**	**MW218089**	DQ094587	DQ236629	**MW218135**	EU329625	DQ247128
	CBS 143226	USA	Kemps Ridley turtle	**MW218044**	**MW218090**	KC808244	MG189922	**MW218136**	KC808342	KC808202
Neocosmospora spathulata	CBS 145474^{T}	USA	Human synovial fluid	**MW218045**	**MW218091**	EU329674	EU329674	**MW218137**	EU329542	DQ246882
Neocosmospora stercicola	CBS 142481^{T}	Germany	Compost yard debris	-	-	LR583779	LR583984	-	LR583887	LR583658
	CBS 144388	Belgium	Greenhouse humic soil	-	-	LR583780	LR583985	-	LR583888	LR583659
Neocosmospora suttoniana	CBS 143214^{T}	USA	Human wound	**MW218046**	**MW218092**	DQ094617	DQ236659	**MW218138**	EU329630	DQ247163
	CBS 143224	USA	Equine eye	**MW218047**	**MW218093**	MG189940	MG189925	**MW218139**	KC808336	KC808197
Neocosmospora tonkinensis	CBS 115.40^{T}	Vietnam	*Musa sapientum*	**MW218048**	**MW218094**	MG189941	MG189926	**MW218140**	LT960564	LT906672
	CBS 118931	UK	*Solanum lycopersicum*	**MW218049**	**MW218095**	LR583784	LR583989	**MW218141**	LR583891	LR583662
Neocosmospora vasinfecta	CBS 446.93	Japan	Soil	-	-	LR583791	LR583996	-	LR583898	LR583670
	CBS 533.65	India	Unknown	-	-	LR583792	LR583997	-	LR583899	LR583671

[1] CBS: Westerdijk Fungal Biodiverity Institute (WI), Utrecht, The Netherlands; CPC: Collection of P.W. Crous, held at WI; NRRL: Agricultural Research Service Culture Collection, National Center for Agricultural Utilization Research, USDA, Peoria, IL, USA; VG: Working collection of J. Van Niekerk held at Department of Plant Pathology, University of Stellenbosch, South Africa; ET: Ex-epitype, IT: Ex-isotype, NT: Ex-lectotype.

[2] *acl*: ATP citrate lyase largest subunit; *cal*: calmodulin; ITS: internal transcribed spacer region of the rDNA; LSU: large subunit of the rDNA; *rpb1*: RNA polymerase largest subunit; *rpb2*: RNA polymerase second largest subunit; *tef1*: translation elongation factor 1-alpha. Sequences generated in the present study are shown in **bold font**.

mined as putative novel species in the previous analyses. For RAxML analyses, the default parameters were selected and clade stability was determined by bootstrap (BS) analysis using 1000 repetitions. Bayesian analyses consisted of two parallel runs of 5 M generations, with the stop-rule on, set to 0.01. The sampling frequency was set to 1000 generations, and consensus trees and posterior probability values (PP) were calculated after discarding the first 25% of sampled trees as the burn-in fraction. The best evolutionary model for each gene partition was determined using MrModelTest v. 2.3 (Nylander, 2004).

RESULTS

Sampling, fungal collection and isolation

In the Patensie and Kirkwood areas, diseased trees initially showed yellowing, wilting leaves and dieback of branch tips. Symptoms subsequently progressed with defoliation and sudden decline before the plants died. Inspection of affected trees showed cracks or blisters on the trunks above the crowns with, rarely, gum exudates (Figure 1). If each trunk was transversely cut, brown to black discolouration and necrosis of the vascular tissue became visible with different extensions (Figure 2). Similar discolouration and stains were visible into the scaffold roots. Symptoms were observed in orchards older than 8 years. Incidence of symptomatic plants was in some cases up to 50% of affected trees in orchards.

A total of 62 monosporic isolates resembling those of *Neocosmospora* were collected from the sampled citrus trees. Among them, 33 isolates were obtained from the Kirkwood area and 29 from Patensie. Thirty-eight were isolated from trunk portions, 22 from scaffold roots, and two from soil surrounding infected roots. Among the isolates collected from trunks, 17 were from necrotic tissue, two from healthy tissue and 14 from the margins between necrotic and healthy tissues.

Phylogenetic studies and identification of the pathogens

A first analysis, based on combined *rpb2* and *tef1* loci, was conducted to identify the *Neocosmospora* isolates obtained from symptomatic citrus trees. The dataset contained 129 isolates, representing 62 South African isolates, as well as 67 ex-type or reference strains representing 46 taxa in *Neocosmospora,* and two outgroup taxa (*Geejayessia atrofusca* NRRL 22316 and *G. cicatricum* CBS 125552). The alignment included 2290 positions (1614 *rpb2*, 676 *tef1*) of which 748 were variable (480 *rpb2*, 268 *tef1*), and 562 positions were phylogenetically informative sites (379 *rpb2*, 183 *tef1*). For both gene partitions, a GTR + I + G model was selected and incorporated in the analyses. The BI lasted for 1,855,000 generations, and the consensus tree and PP were calculated from 1392 trees after discarding 494 trees as burn-in fraction. Phylogenetic trees inferred using ML and BI analyses resulted in very similar topologies, and therefore only the ML tree is presented in Figure 3a. The South African isolates were distributed among 11 distinct phylogenetic lineages, of which seven corresponded to known *Neocosmospora* species, which were, in order of frequency of isolation: *N. ferruginea* and *N. solani* (15 isolates each), *N. hypothenemi* (five isolates), *N. brevis* (three isolates), *N. noneumartii* (two isolates), and *N. crassa* and *N. falciformis* (one isolate each). The remaining 20 South African isolates grouped within four undescribed phylogenetic lineages, among which 15 isolates clustered in a well-supported clade ("*Neocosmospora* sp. 1", BS = 93/PP = 0.96), sister to *N. bataticola*; three isolates (VG268, 279 and 281) clustered in a fully-supported clade ("*Neocosmospora* sp. 2", BS = 100/PP = 100), sister to *N. metavorans*; while two isolates (singletons VG16 and VG48) were resolved as single lineages (respectively, "*Neocosmospora* sp. 3" and "*Neocosmospora* sp. 4"); however, with low statistical support values compared with those in the *rpb2* and *tef1* analyses.

To further assess the phylogenetic position of the putative novel phylogenetic clades, a second, more robust multi-locus phylogenetic analysis was performed using seven loci (*acl*, *cal*, ITS, LSU, *rpb1*, *rpb2* and *tef1*) and selected strains representing closely related species, as determined in the previous phylogenetic assessment of the genus *Neocosmospora*. The combined dataset included 5904 positions (616 *acl*, 573 *cal*, 467 ITS, 480 LSU, 1489 *rpb1*, 1613 *rpb2* and 666 *tef1*) from 47 strains, representing a subset of 28 phylogenetic clades of *Neocosmospora*, plus two outgroup taxa. From the total sites included, 1405 were variable (188 *acl*, 103 *cal*, 100 ITS, 34 LSU, 372 *rpb1*, 390 *rpb2* and 218 *tef1*), and 856 were phylogenetically informative (81 *acl*, 82 *cal*, 70 ITS, 22 LSU, 196 *rpb1*, 266 *rpb2* and 139 *tef1*). Optimal model selection for each gene partition was determined as follows: GTR + G for *tef1*, GTR + I + G for LSU and ITS; K80 + G for *acl*, K80 + I + G for *cal*, and SYM + I + G for *rpb1* and *rpb2*. The BI lasted for 1,520,000 generations, and PP were calculated from 1141 trees after discarding 380 trees as the burn-in fraction. The BI analysis (shown in Figure 3 b) confirmed the topology obtained by ML.

The analyses confirmed the results obtained in the two-gene phylogeny, and the four novel lineages were resolved with high BS and PP support. *Neocosmospora* sp. 2 and representative isolates of clade *Neocosmospora*

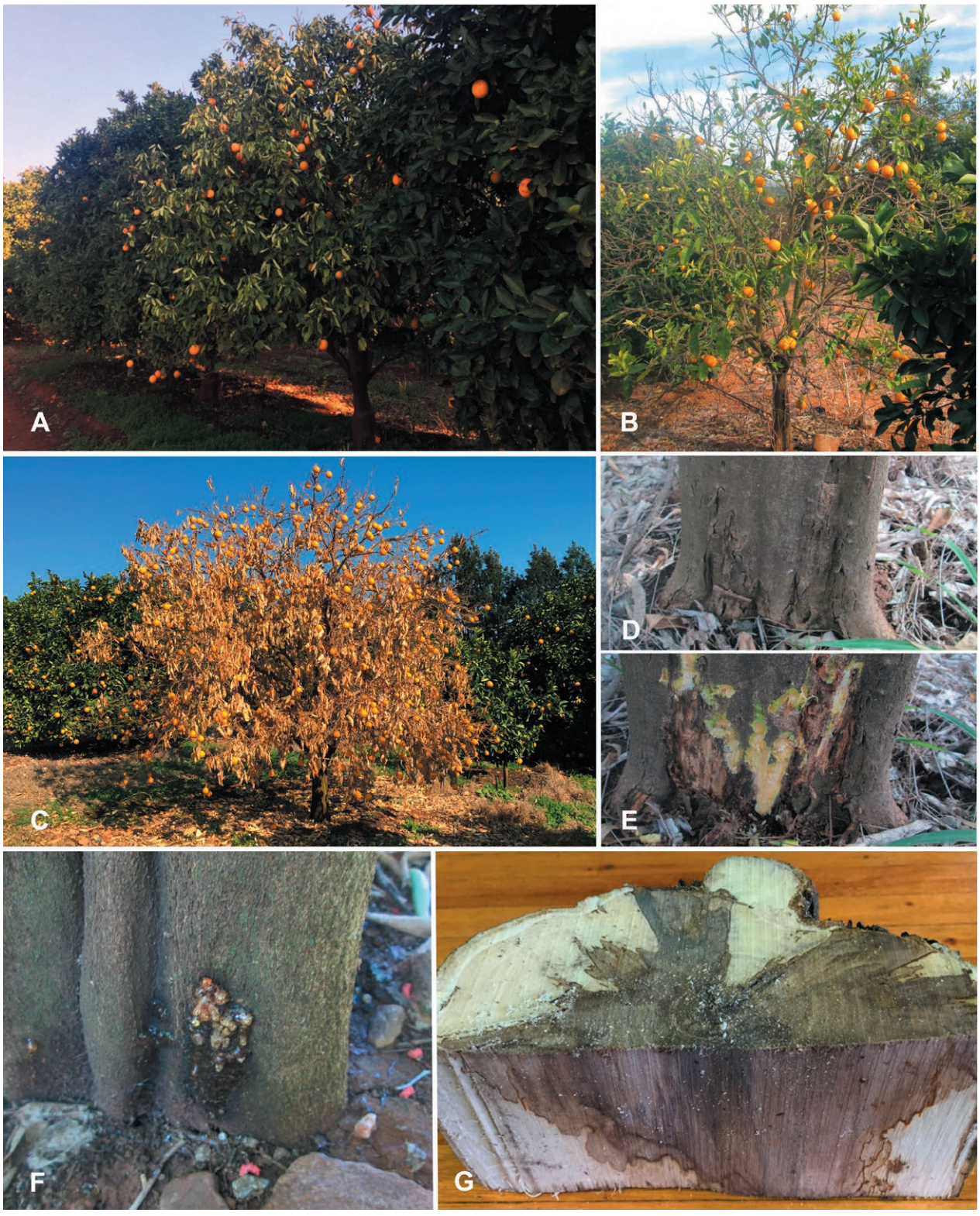

Figure 1. Dry root rot symptoms of citrus observed in South Africa. Tree decline progression: initial leaves wilting (A), yellowing, loss of leaves, and dieback of branch tips (B) and plant death (C). External cracks or blisters on the trunk portion above the crown (D) and internal dry rot (E) of the same plant. Gum exudate at the crown level (F). Brown to black discolouration and necrosis of the vascular tissue visible in longitudinal and transverse sections (G).

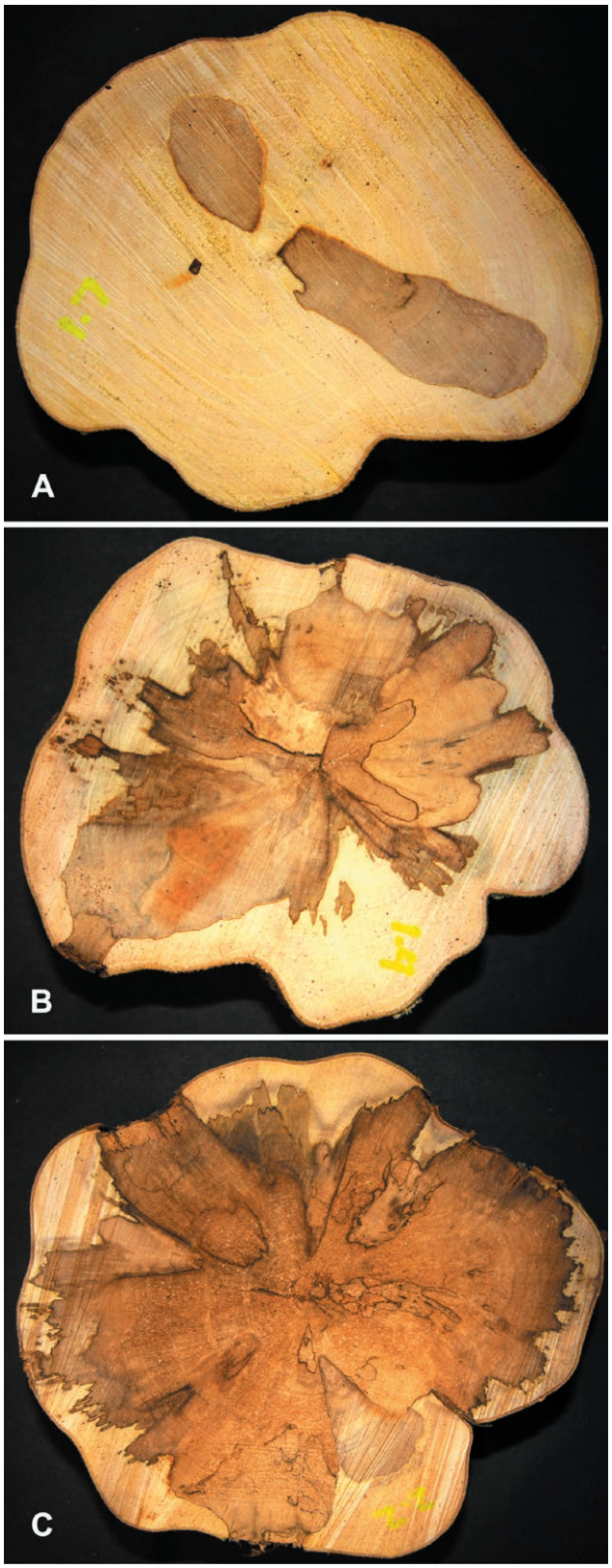

Figure 2. Small (A), medium (B) or large (C) extensions of internal discolouration in transverse sections through citrus tree trunks.

sp. 1 were both resolved as fully supported clades (BS = 100/PP = 100), while the lone lineages *Neocosmospora* sp. 3 and *Neocosmospora* sp. 4 were confidently resolved as well-supported branches (respectively, BS = 96/PP = 0.97 and BS = 86/PP = 0.96). These four phylogenetic lineages are therefore here proposed as the novel species *Neocosmospora addoensis*, *N. citricola*, *N. gamtoosensis* and *N. lerouxii*.

Taxonomy

Neocosmospora addoensis Sand.-Den. & Guarnaccia, *sp. nov.* – MycoBank MB837939; Figure 4.

Etymology. Named after the geographical area Addo, South Africa where first collected.

Typus. South Africa, Eastern Cape, Kirkwood, from *Citrus sinensis* crown, May 2018, *V. Guarnaccia* (holotype CBS H-24565 designated here, culture ex-type CBS 146510 = CPC 37128 = VG281).

Conidiophores borne on aerial mycelium, 53.5–425 µm long, unbranched or less commonly laterally branched, bearing terminal single phialides, proliferating percurrently; aerial phialides monophialidic, subulate to subcylindrical, smooth- and thin-walled, 34–64.5 × 2–4 µm, with short and flared apical collarettes and inconspicuous periclinal thickening; *aerial conidia* arranged in false heads on phialide tips, hyaline, broadly ellipsoidal to clavate and slightly asymmetrical, smooth- and thin-walled, aseptate, (5.5–)7–10(–14.5) × (2–)3–4 µm (av. 8.5 × 3 µm). *Sporodochia* pale luteous to pale peach coloured, formed abundantly on carnation leaves. *Sporodochial conidiophores* unbranched or laterally and irregularly branched bearing apical groups of 2–3 monophialides; *sporodochial phialides* subulate to subcylindrical, 12.5–25 × 2–4.5 µm, smooth and thin-walled, commonly proliferating sympodially, collarettes and periclinal thickening absent or inconspicuous. *Sporodochial conidia* falcate, slightly curved dorsoventrally to almost straight, broadest near the half portion or the upper third, tapering towards both ends, with blunt and slightly curved apical cells and blunt, sometimes inconspicuous foot-like basal cells, (1–)2–5-septate, predominantly 4-septate, hyaline, smooth- and thick-walled; one-septate conidia: (18.5–)19–24(–25) × 3–4.5 µm (av. 21.5 × 4 µm); two-septate conidia: (24–)26–30 × 3.5–5 µm (av. 27.5 × 4.5 µm); three-septate conidia: (27–)33–43(–45) × (3–)4–5.5(–6) µm (av. 38 × 5 µm); four-septate conidia: (39–)42–47.5(–51.5) × 4.5–6 µm (av. 49 × 5.5 µm); five-septate conidia: (37.5–)42.5–51 × 5–6 µm (av. 47 × 5.5 µm). *Chlamydospores* subspherical to spherical, hyaline to pale yellow, smooth-walled or slightly roughened, thick-walled, 4–10 µm, single or in chains, terminal or intercalary on hyphae and conidia.

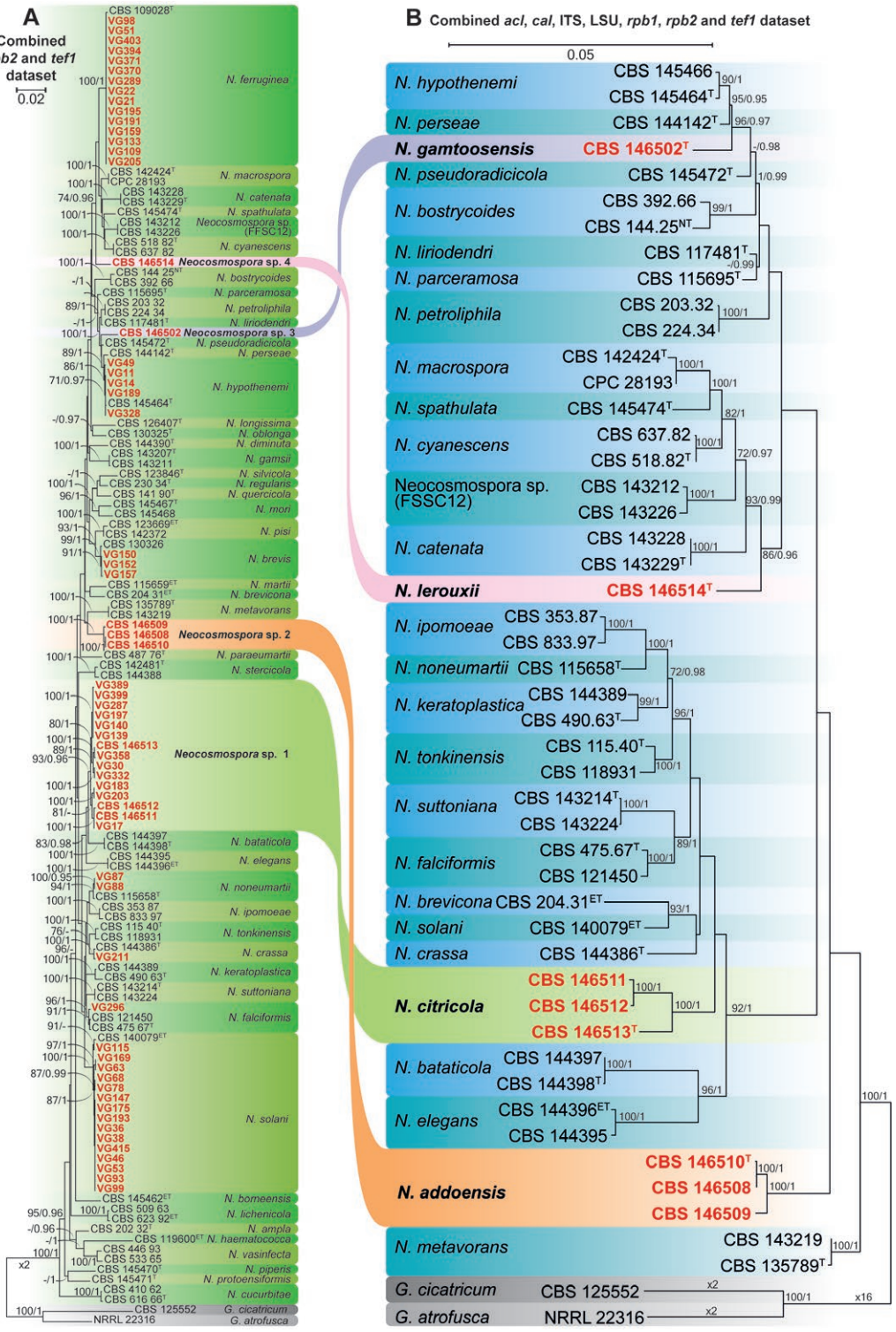

Figure 3. Maximum-likelihood (ML) phylograms obtained from combined *rpb2* and *tef1* (A) and *acl*, *cal* ITS, LSU, *rpb1*, *rpb2* and *tef1* (B) sequences, of 62 isolates of *Neocosmospora* spp. from South African *Citrus* (shown in red), and representative and ex-type isolates of *Neocosmospora*. Names of new species described here are shown in **bold font**. Numbers on the nodes are ML bootstrap values greater than 70% followed by Bayesian posterior probability values greater than 0.95. Branch lengths are proportional to distance. Ex-type, ex-epitype and ex-neotype strains are indicated, respectively, with ^{T}, ^{ET} and ^{NT}. The trees are rooted to *Geejayesia atrofusca* (NRRL 22316 and *G. cicatricum* (CBS 125552).

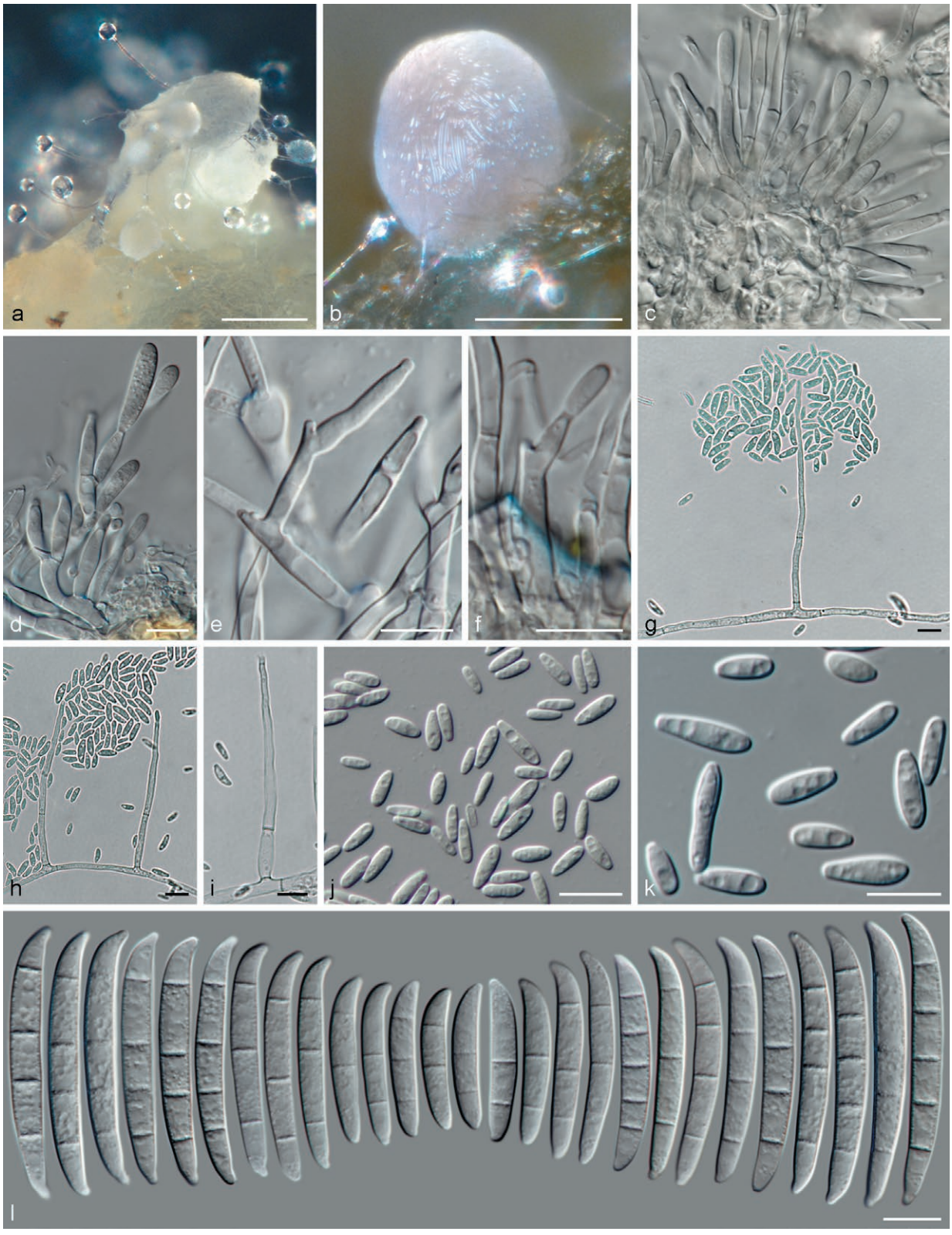

Figure 4. *Neocosmospora addoensis* (ex-type culture CBS 146510). (a and b) sporodochia formed on the surface of carnation leaves; (c to f) sporodochial conidiophores and phialides; (g to i) aerial conidiophores; (j and k. aerial conidia; (l) sporodochial conidia. Scale bars: a and b = 100 µm; c to l = 10 µm.

Culture characteristics. Colonies on PDA reaching 79 mm diam. at 24°C after 7 d (growth rate: 4.1–5.6 mm d^{-1}). Colony surface white to primrose, becoming scarlet to bay, flat with abundant dense aerial mycelium, cottony to woolly; colony reverse pale luteous to sulphur yellow, a vivid scarlet to rust pigment can be formed. On SNA, white to pale buff, membranous to woolly with scant aerial mycelium, becoming powdery; colony reverse white to pale buff. On OA, pale luteous to pale rosy buff, flat, membranous to cottony; colony reverse pale luteous to pale rosy buff.

Additional materials examined. South Africa, Eastern Cape, Patensie, from *Citrus sinensis* crown, May 2018, *V. Guarnaccia* (CBS 146508 = CPC 37126 = VG 268, CBS 146509 = CPC 37127 = VG279).

Notes. Both phylogenetic analyses resolved *Neocosmospora addoensis* as the closest genetic relative to *N. metavorans* (96 to 98% sequence similarity among individual gene datasets). *Neocosmospora metavorans* is a frequent opportunistic pathogen of animals, including humans (Sandoval-Denis *et al*., 2019). Nevertheless, in addition to its genetic exclusivity, these two species are morphologically quite distinct, particularly in the size and septation of the aerial conidia (aseptate, up to 14.5 µm in *N. addoensis* and multiseptate, up to 25 µm in *N. metavorans*), while sporodochial conidia of *N. addoensis* are more slender (up to 6 µm wide) than those of *N. metavorans* (up to 7.5 µm wide).

Neocosmospora addoensis is characterized by its small and slender macroconidia, which are much smaller than the average macroconidial type in *Neocosmospora*. Based on its macroconidial size, this species is close to *N. brevis* and *N. pseudoradicicola*; however, these two species are well-delimited phylogenetically, clustering in far separate lineages of the genus (96% sequence similarity with *N. brevis* and 97% with *N pseudoradicicola*). Morphologically, *N. addoensis* differs from *N. pseudoradicicola* by its macroconidial shape and curvature, with more rounded apical cells, rather inconspicuous foot cells and less pronounced dorsoventral curvature; and from *N. brevis* by the absence of aerial macroconidia and slightly more elongated and hooked macroconidial apical cells.

Neocosmospora citricola Guarnaccia & Sand.-Den., *sp. nov.* – MycoBank MB837940; Figure 5.

Etymology. In reference to occurrence of this fungus on *Citrus* plants.

Typus. South Africa, Eastern Cape, Patensie, from *Citrus sinensis* crown, May 2018, *V. Guarnaccia* (holotype CBS H-24566 designated here, culture ex-type CBS 146513 = CPC 37131 = VG343).

Conidiophores borne on aerial mycelium, 66.5–198.5 µm long, unbranched or irregularly laterally branched, bearing terminal single phialides; *aerial phialides* monophialidic, subulate to subcylindrical, smooth- and thin-walled, 39.5–73.5 × 2–4.5 µm, each showing a discrete flared collarette and inconspicuous to evident periclinal thickening; *aerial conidia* arranged in false heads on phialide tips, hyaline, broadly ellipsoidal to obovoidal, rarely clavate, smooth- and thin-walled, 0–1-septate, (6–)9–17(–24.5) × 3–5(–6.5) µm (av. 13 × 4.5 µm). *Sporodochia* pale luteous to pale orange, formed abundantly on carnation leaves and on the agar surface. *Sporodochial conidiophores* laterally and irregularly branched, bearing single terminal monophialides or terminal groups or up to three monophialides; *sporodochial phialides* subulate to subcylindrical, 11–27.5 × 3–5.5 µm, smooth and thin-walled, with inconspicuous or absent apical collarettes and periclinal thickening. *Sporodochial conidia* falcate, curved dorsoventrally to almost straight, each with broadening in the upper third, tapering towards both ends, with a blunt to papillate and slightly curved apical cell and a blunt, foot-like basal cell, (2–)3–5(–6)-septate, predominantly five-septate, hyaline, robust, smooth- and thick-walled; two-septate conidia, 44 × 5.7 µm; three-septate conidia: 33.5–49.5(–58) × 4.5–6 µm (av. 43 × 5.5 µm); four-septate conidia: (46.5–)47.5–56(–59.5) × 5–6.5 µm (av. 52 × 6 µm); five-septate conidia: (49.5–)53–60.5(–65) × (4.5–)5.5–6.5(–7) µm (av. 57 × 6 µm); six-septate conidia: 60 × 6 µm. *Chlamydospores* subspherical to spherical, hyaline to pale golden brown, smooth to slightly roughened and thick-walled, 5–10 µm, single or in chains, terminal or intercalary on hyphae and conidia.

Culture characteristics: Colonies on PDA reaching 69 mm diam. at 24°C after 7 d (growth rate: 3.2–4.9 mm d^{-1}). Colony surfaces straw, buff to pale luteous, with pale luteous to orange centres and abundant aerial mycelium, flat, felty, woolly to cottony with abundant concentric rings of aerial mycelium, colony reverse pale luteous to orange. On SNA, white and translucent, flat, woolly, becoming slightly pulverulent with sporulation, colony reverse white. On OA, saffron to peach, flat, membranous to cottony, colony reverse intense peach to flesh.

Additional materials examined. South Africa, Eastern Cape, Patensie, from *Citrus sinensis* crown, May 2018, *V. Guarnaccia* (CBS 146511 = CPC 37129 = VG302, CBS 146512 = CPC 37130 = VG307).

Notes. *Neocosmospora citricola* resolved as a highly supported monophyletic clade, basal to a fully supported lineage containing *N. bataticola* and *N. elegans*, which clearly differentiated genetically (96 to 98% sequence similarity to *N. citricola* in the single gene datasets).

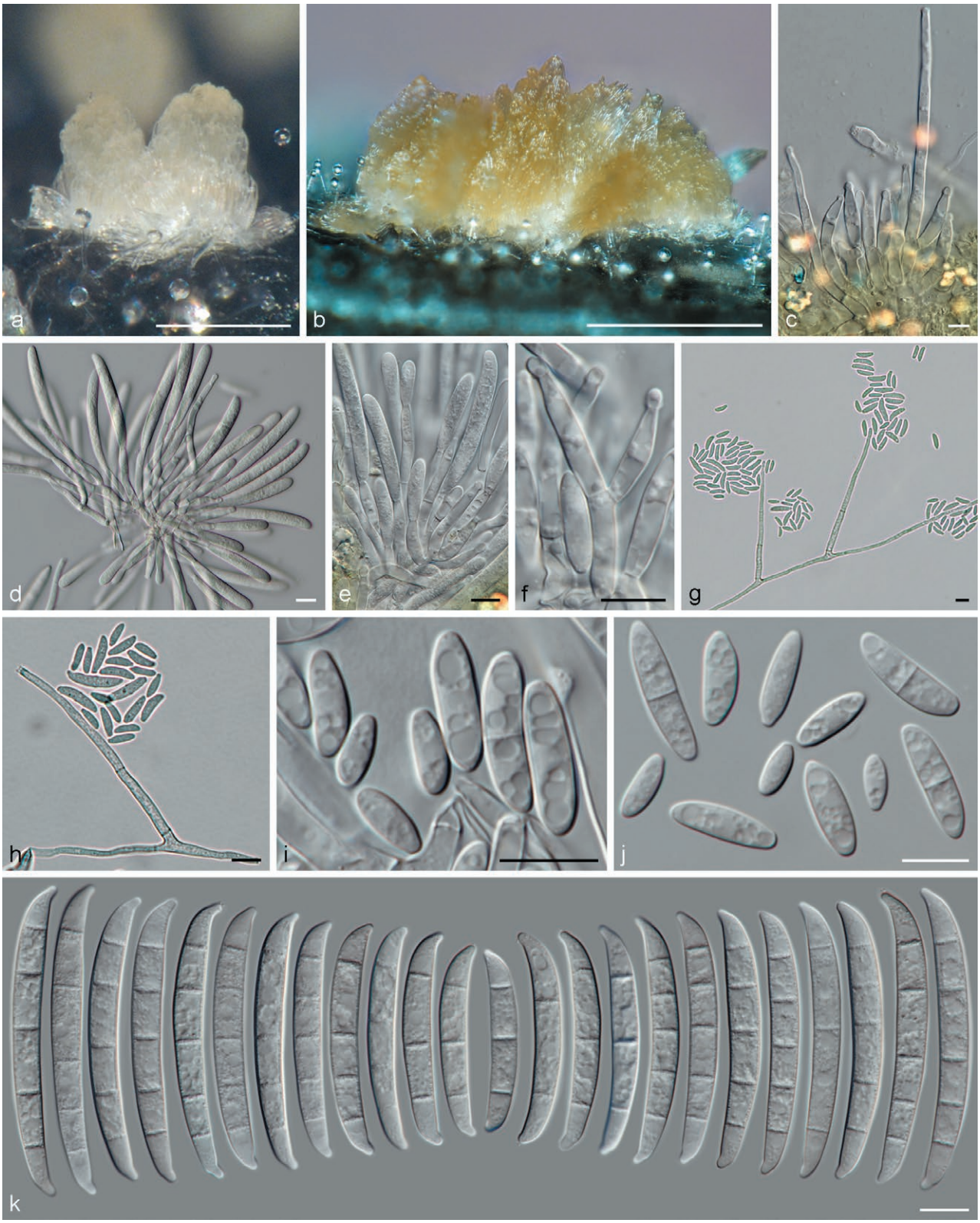

Figure 5. *Neocosmospora citricola* (ex-type culture CBS 146513). (a and b) sporodochia formed on the surface of carnation leaves; (c to f) sporodochial conidiophores and phialides; (g and h) aerial conidiophores;(I and j) aerial conidia; (k) sporodochial conidia. Scale bars: a and b = 100 µm; c to k = 10 µm.

Although genetically distant, *Neocosmospora citricola* is morphologically similar to *N. nirenbergiana*, *N. piperis* and *N. protoensiformis* (92% sequence similarity with *N. nirenbergiana* and 96% with *N. piperis* and *N. protoensiformis*; data not shown), the four species producing very similar macroconidia in shape and overall size. Nevertheless, *N. citricola* differs from *N. nirenbergiana* and *N. piperis* by the absence of aerial macroconidia. Conversely, *N. nirenbergiana* and *N. piperis* do not produce aerial microconidia, and the aerial conidiophores of *N. citricola* are much more robust than those of *N. nirenbergiana* and *N. piperis*. *Neocosmospora protoensiformis* also lacks aerial macroconidia; however, in addition to forming smaller microconidia (up to 15 µm long, average size 7.6 × 3.6 µm in *N. protoensiformis vs* up to 24 µm long, average size 13 × 4.5 µm in *N. citricola*), and shorter sporodochial phialides (up to 19.5 µm long in *N. protoensiformis vs* up to 27.5 µm long in *N. citricola*), macroconidia of *N. protoensiformis* differ from those of *N. citricola* by usually being more tapered at both ends.

Neocosmospora gamtoosensis Sand.-Den. & Guarnaccia, *sp. nov.* – Mycobank MB837941; Figure 6.

Etymology. Named after the valley where this fungus was collected, Gamtoos River Valley, South Africa.

Typus. South Africa, Eastern Cape, Patensie, from *Citrus sinensis* crown, May 2018, *V. Guarnaccia* (holotype CBS H-24564 designated here, culture ex-type CBS 146502 = CPC 37120 = VG16).

Conidiophores borne on aerial mycelium, 96.5–291 µm long, unbranched or irregularly laterally branched, bearing terminal single phialides; *aerial phialides* monophialidic, subulate to subcylindrical, smooth- and thin-walled, 17.5–61 × 2–3.5 µm, collarettes and periclinal thickening evident; *aerial conidia* arranged in false heads on phialide tips, hyaline, broadly ellipsoid, obovoid to short clavate, smooth- and thin-walled, aseptate, (4.5–)5.5–9(–11.5) × 2–3.5(–6) µm (av. 7 × 3 µm). *Sporodochia* citrine to honey, formed abundantly on carnation leaves. *Sporodochial conidiophores* commonly unbranched and densely packed, bearing terminal, single monophialides or groups of 2–3 phialides; *sporodochial phialides* lageniform to ampulliform, 7.5–17 × 3–5 µm, smooth and thin-walled, each with an often conspicuous periclinal thickening and a reduced, flared collarette. *Sporodochial conidia* falcate, slightly curved dorsoventrally to almost straight on their ventral faces, broadening in the upper third, tapering towards both ends, with blunt and hooked apical cells and blunt to slightly pointed and extended foot-like basal cells, (4–)5–6(–7)-septate, predominantly five-septate, hyaline, smooth- and thick-walled; four-septate conidia: (37–)40–55(–56.5) × 4.5–5.5 µm (av. 48.5 × 5 µm); five-septate conidia: (46.5–)51.5–60(–62) × 4.5–5.5 µm (av. 56 × 5 µm); six-septate conidia: 55.5–64(–65) × 4.5–5.5 µm (av. 60 × 5 µm); seven-septate conidia: 60.5 × 5 µm. *Chlamydospores* subspherical, hyaline to pale yellow, inconspicuously roughened, thick-walled, 5–12 µm diam., single or forming chains or clusters, terminal or intercalary on hyphae.

Culture characteristics: Colonies on PDA reaching 60 mm diam. at 24°C after 7 d (growth rate: 3.8–4.3 mm d^{-1}). Colony surfaces pale luteous, amber to pure yellow, flat with abundant dense aerial mycelium in radial patches, cottony to woolly, colony reverse pale luteous to vivid pure yellow. On SNA, colonies white to pale buff, translucent, flat, woolly with scant aerial mycelium, becoming slightly powdery; reverse white to pale buff. On OA, the colonies are pale luteous, pale buff to primrose, flat, membranous to cottony, and colony reverse pale luteous to pale rosy buff.

Notes. In the combined *rpb2* and *tef1* analysis, *Neocosmospora gamtoosensis* formed an unsupported lone lineage, basal to a larger lineage containing *N. hypothenemi*, *N. perseae* and *N. pseudoradicicola*. The combined seven-loci analysis resolved *N. gamtoosensis* within the larger lineage, with high statistical support for all the earlier listed species. Base pair similarities between the novel species and its closest relatives ranged from 98% in the combined dataset to between 96 and 99% in the individual gene datasets.

Neocosmospora gamtoosensis is morphologically reminiscent of *N. hypothenemi*, both species having predominantly five-septate macroconidia of very similar size and shape; however, *N. gamtoosensis* has conspicuously flared collarettes on its aerial phialides, also producing shorter (length up to 11.5 µm, average = 7 µm in *N. gamtoosensis vs* up to 13.5 µm, average = 8.2 µm in *N. hypothenemi*), aseptate aerial conidia, and honey coloured sporodochia (yellow-green in *N. hypothenemi*), and lacking reddish pigments on PDA. *Neocosmospora noneumartii*, another genetically distant (97% sequence similarity in the combined analysis), but morphologically similar species, differs from *N. gamtoosensis* by forming dimorphic conidia from aerial phialides and longer sporodochial conidia (five-septate sporodochial conidia of average length 56 µm *vs* 63 µm in *N. noneumartii*). *Neocosmospora gamtoosensis* is also morphologically very similar to *N. lerouxii*. However, *N. gamtoosensis* has shorter (five-septate sporodochial conidia average length 63 µm in *N. lerouxii*) and more curved sporodochial conidia.

Neocosmospora lerouxii Guarnaccia & Sand.-Den., *sp. nov.* – Mycobank MB837942; Figure 7.

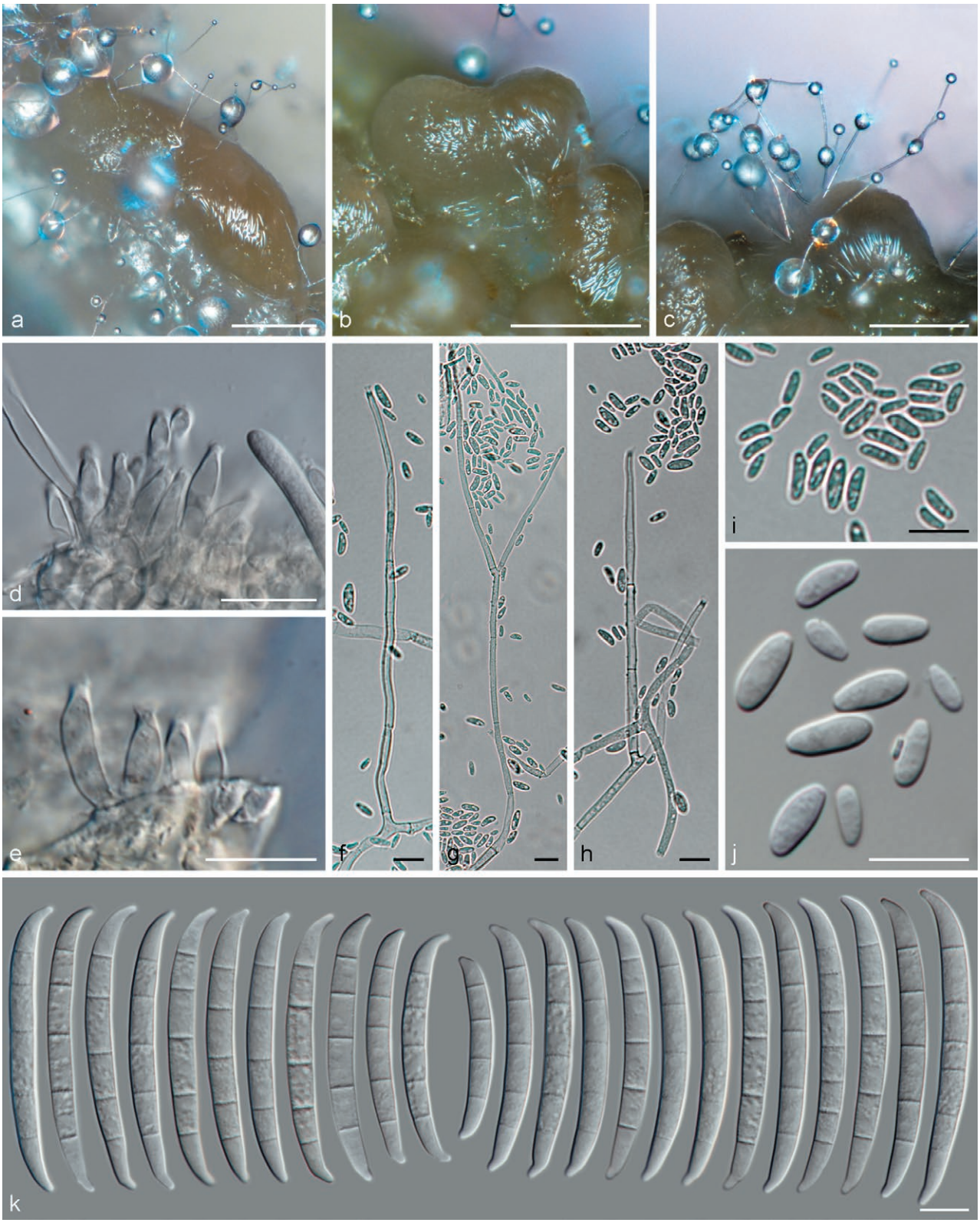

Figure 6. *Neocosmospora gamtoosensis* (ex-type culture CBS 146502). (a toc) sporodochia formed on the surface of carnation leaves; (d and e) sporodochial conidiophores and phialides; (f to h) aerial conidiophores; (I and j) aerial conidia; (k) sporodochial conidia. Scale bars: a and b = 100 µm; c to k = 10 µm.

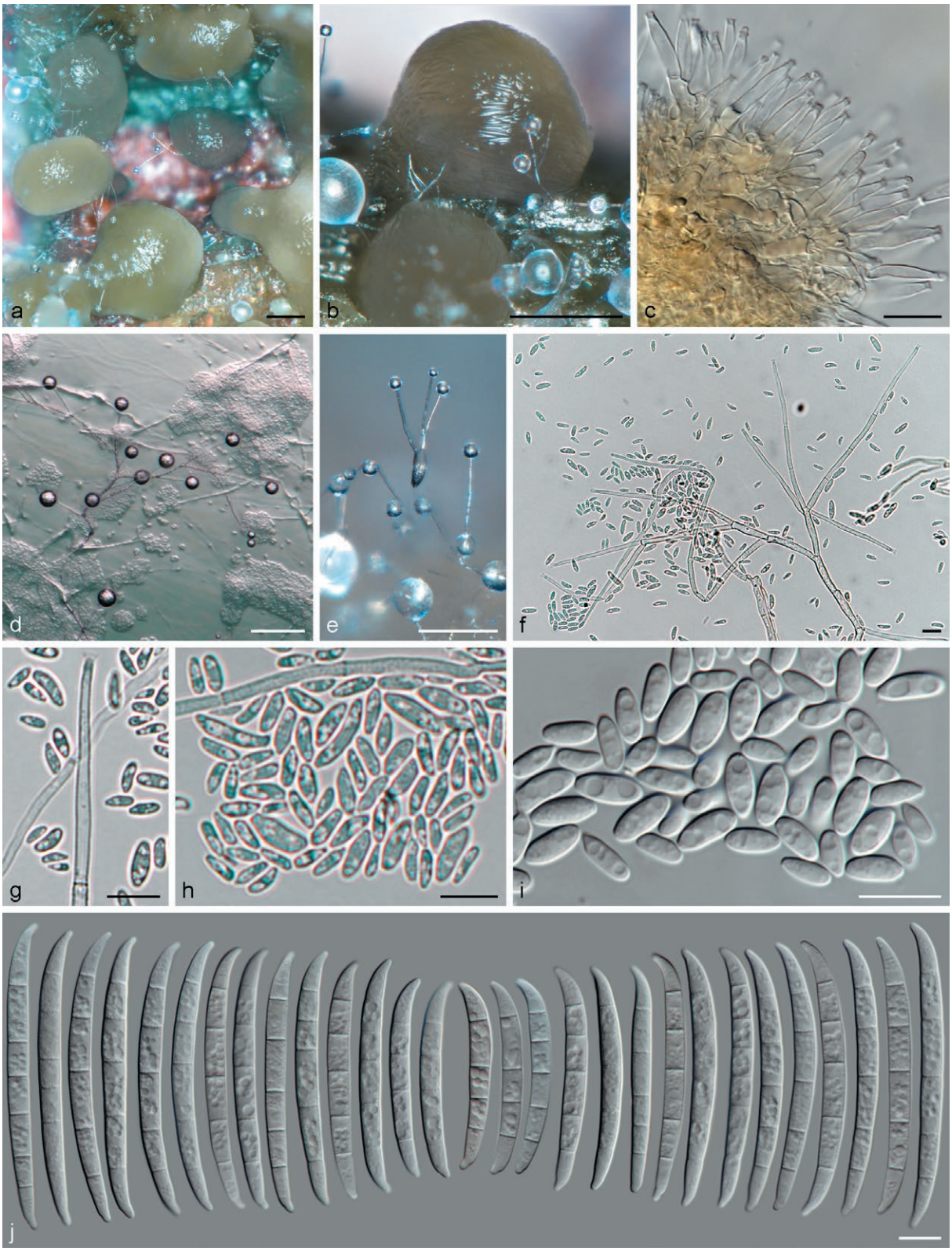

Figure 7. *Neocosmospora lerouxii* (ex-type culture CBS 146514). (a and b) sporodochia formed on the surface of carnation leaves; (c) sporodochial conidiophores and phialides; (d tog) aerial conidiophores and phialides; (h and i) aerial conidia; (j) sporodochial conidia. Scale bars: a and b = 100 µm; d and e = 50 µm; f to j = 10 µm.

Etymology. In memory of Dr Hennie Le Roux (10 Jul 1967 – 4 Oct. 2016), who made major contributions to the South African and international citrus industries.

Typus. South Africa, Eastern Cape, Patensie, from *Citrus sinensis* root scaffold, May 2018, *V. Guarnaccia* (holotype CBS H-24567 designated here, culture ex-type CBS 146514 = CPC 37132 = VG48).

Conidiophores borne on aerial mycelium, 139.5–295 µm long, simple or most commonly abundantly and irregularly branched, proliferating percurrently, bearing terminal single phialides; *aerial phialides* monophialidic, subulate to subcylindrical, smooth- and thin-walled, 37–61.5 × 2–4 µm, with periclinal thickening and collarettes abundant; *aerial conidia* arranged in false heads on phialide tips, hyaline, ovate, broadly ellipsoidal to short clavate, smooth- and thin-walled, 0(–1)-septate, (4.5–)6–10(–18.5) × 2–5 µm (av. 8 × 3.5 µm). *Sporodochia* pale luteous, ochreous to citrine, formed abundantly on carnation leaves and on agar surfaces. *Sporodochial conidiophores* verticillately and laterally branched and densely packed, smooth- and thin-walled, bearing apical whorls of up to four monophialides; *sporodochial phialides* subulate to subcylindrical, (12–)14.5–19.5(–22.5) × 2.5–4.5 µm, smooth- and thin-walled, with conspicuous periclinal thickening and short, flared collarettes. *Sporodochial conidia* falcate, almost straight or gently curved dorsiventrally, each broadening in the centre and upper third, tapering towards both ends, with a conical and slightly curved apical cell and a notched foot-like basal cell, (2–)4–6-septate, predominantly five-septate, hyaline, smooth- and thick-walled; two-septate conidia, 29 × 4 µm; three-septate conidia: 40 × 5 µm; four-septate conidia: (44–)45–49(–50.5) × (4–)4.5–5 µm (av. 47 × 5 µm); five-septate conidia: (46.5–)56.5–67(–73.5) × 4.5–5(–6.5) µm (av. 62 × 5 µm); six-septate conidia: 60–74 × 4.5–5.5 µm (av. 67 × 5 µm). *Chlamydospores* subspherical to spherical, hyaline to pale yellow-brown, smooth- and thick-walled, 4–8 µm diam., single or in chains, terminal or intercalary on hyphae.

Culture characteristics. Colonies on PDA reaching 61 mm diam. at 24°C after 7 d (growth rate: 3.5–4.3 mm d^{-1}). Surfaces buff, pale luteous to pale flesh, with abundant and dense whitish aerial mycelium, flat to slightly raised, felty to cottony. Colony reverse pale luteous, quickly becoming amber to sulphur yellow, with or without pale apricot patches. On SNA, colonies white and translucent, flat, felty, with white reverse sides. On OA, colonies white, saffron to buff, flat, membranous to cottony, with reverse sides buff to pale luteous with pale salmon patches.

Notes. The combined *rpb2* plus *tef1* analysis showed this taxon to form a well-supported (BS = 74, PP = 0.96) lone lineage, basal to a larger, unsupported linage containing *N. catenata*, *N. cyanescens*, *N. ferruginea*, *N. macrospora*, and *N. spathulata*, and the undescribed phylogenetic species FSSC 12. The analysis of the combined seven-gene dataset confirmed the previous results, with all the species described here resolved as highly- to fully-supported monophyletic clades. Genetic similarity between *N. lerouxii* and its closest phylogenetic relatives also support phylogenetic exclusivity of *N. lerouxii* (98% sequence similarity with all the above taxa in the combined alignment, and 97 to 99% similarity for the individual gene datasets).

Morphologically, *Neocosmospora lerouxii* most closely resembles the three distantly related species *N. gamtoosensis*, *N. hypothenemi* and *N. noneumartii* (respectively, 97, 98 and 97% sequence similarity, in the seven-loci combined dataset). While the three species were clustered in well-separated lineages in all analyses, morphologically they share very similar characteristics. Although *N. lerouxii* has similar macroconidial shape to *N. gamtoosensis* and *N. hypothenemi*, the macroconidia of *N. lerouxii* are longer and straighter than in the other two species (five-septate macroconidia average length 62 µm *vs* 56 µm in *N. gamtoosensis* and 59 µm in *N. hypothenemi*). Macroconidia of *N. lerouxii* also have thinner walls in comparison to those of *N. noneumartii*. In addition, has a slower growth rate in culture than *N. noneumartii*, (3.5–4.3 mm d^{-1} for *N. lerouxii vs* 4.7–8 mm d^{-1} in *N. noneumartii*).

DISCUSSION

Since 2013, severe sudden decline and death of citrus plants has been observed in citrus production areas of the Eastern Cape province of South Africa. Several species of *Colletotrichum*, *Diaporthaceae* and *Botryosphaeriaceae* have been reported as causing wood decay of citrus plants internationally (Guarnaccia and Crous, 2018; Mayorquin *et al*., 2019; Berraf-Tebbal *et al*., 2020; Esparham *et al*., 2020; Bezerra *et al*., 2021). Considering the very large economic losses to the South African citrus industry due to the observed sudden decline of trees, and because no surveys and isolations had been previously conducted for this disease and associated pathogens in the Eastern Cape citrus production area, a large-scale survey of affected citrus plants was required. The present study provides the first preliminary survey and sampling of citrus trees affected by dry root rot, and characterization of *Neocosmospora* diversity related to the observed disease in two important citrus production areas of South Africa.

Neocosmospora species are well-established in geographical areas with Mediterranean, sub-tropical or tropical climates, where these fungi are associated with diseases of important agricultural crops (Sandoval-Denis *et al*., 2018; Guarnaccia *et al*., 2018; 2019).

Fusarium oxysporum, *F. proliferatum* and *N. solani* s. str. were previously considered as pathogens associated with dry root rot of citrus plants. (Menge, 1988; Adesemoye *et al*., 2011). Specifically *F. oxysposrum* and *N. solani* were previously reported from South Africa. Diversity of *Fusarium* (three species) and *Neocosmospora* (five species) was revealed associated with dry root rot in restricted areas of three European countries by Sandoval-Denis *et al*. (2018). However, that study considered it likely that many other *Neocosmospora* spp. would also be isolated if a wider sampling area was surveyed.

In the present study, several citrus orchards in two major citrus production area of South Africa were investigated. A total of 62 *Neocosmospora* strains were collected from symptomatic tree trunks, roots and soil surrounding the roots. Phylogenetic analyses as well as morphological characters, revealed ten *Neocosmospora* species associated with infections on *Citrus* in South Africa, plus one species (*N. falciformis*) from soil from affected citrus orchards. The analyses included several of the closest related taxa to each of the *Neocosmospora* species recovered, based on BLAST searches of NCBI's GenBank nucleotide database. The final phylogenetic tree revealed four previously undescribed species (*N. addoensis*, *N. citricola*, *N. gamtoosensis*, *and N. lerouxii*) and six known species (*N. brevis*, *N. crassa*, *N. ferruginea*, *N. hypothenemi*, *N. noneumartii*, and *N. solani*) all of which were always associated with abovementioned symptomatic material.

Neocosmospora citricola, *N. ferruginea* and *N. solani* were the predominant species, largely found associated with the affected tissues of symptomatic plants cultivated in all the investigated orchards. Although follow-up studies will conduct pathogenicity trials to confirm these observations, it is assumed that these species represent the major biotic factors causing DRR of citrus in South Africa as they were consistently associated with the symptoms described from the diseased trees. These results also partially confirm what was recently demonstrated after surveys conducted in Mediterranean countries, where *N. ferruginea* (formerly FSSC28) and *N. solani* were isolated from typical DRR of citrus (Sandoval-Denis *et al*., 2018). *Neocosmospora citricola* was not found before the present study, and considering the broad distribution on affected plants, this fungus is likely to be important in DRR. *Neocosmospora addoensis* was isolated with low frequency, from one orchard and from necrotic trunk tissue. The other novel species described in this study, *N. gamtoosensis and N. lerouxii*, were found only sporadically, and are thus not considered as important pathogens. However, their description provides new insights into the taxonomy of *Neocosmospora*. *Neocosmospora brevis*, *N. crassa*, *N. hypothenemi* and *N. noneumartii* were also isolated sporadically, and future studies will investigate their roles in DRR. The complexity of pathogens associated with artificially reproducing DRR of citrus is well-known (Graham *et al*., 1985), but needs to be confirmed in further field trials. Furthermore, additional surveys in South Africa and other citrus-producing areas, and pathogenicity trials of *Neocosmospora* spp. in association with abiotic factors, should also be conducted.

The present study has provided the first overview of *Neocosmospora* diversity associated with DRR of citrus trees in South Africa, and has given useful information about taxonomic characterization within *Neocosmospora*. All the *Neocosmospora* species were isolated from crowns, trunks, roots and soil from the affected citrus orchards. Infected propagation material and soil can spread the pathogens nationally and internationally as the fungi can survive as chlamydospores in the soil and systemic infections in plant material. Further studies are required to resolve the host range and pathogenicity of all the species recovered. These fungi can survive as endophytes or as latent infections within citrus plants, so healthy propagation material should be used by growers. Favourable climatic conditions and, especially, plant stress factors could also play major roles in disease development. Further research on the epidemiology of DRR of citrus should be conducted to develop specific knowledge as the basis for effective disease prevention and management.

LITERATURE CITED

Adesemoye A.O., Eskalen A., Faber B., Bender G., O'connell N., ... Shea, T. 2011. Current knowledge on Fusarium dry root rot of citrus. *Citrograph* 2: 29–33.

Bender G.S. 1985. Dry Root Rot of Citrus—Factors Which Increase the Susceptibility of Trees to Infection by *Fusarium solani.* PhD dissertation, University of California, Riverside, CA, USA.

Berraf-Tebbal A., Mahamedi A.E., Aigoun-Mouhous W., Špetík M., Čechová J., … Eichmeier A. 2020. *Lasiodiplodia mitidjana* sp. nov. and other *Botryosphaeriaceae* species causing branch canker and dieback of *Citrus sinensis* in Algeria. *PloS one* 15: e0232448.

Bezerra J.D.P, Crous P.W., Aiello D., Gullino M.L., Polizzi G., Guarnaccia V. 2021. Genetic diversity and pathogenicity of *Botryosphaeriaceae* species aassociated with symptomatic citrus in Europe. *Plants* 10: 492.

Broadbent P. 2000. Dry root rot or sudden death. In: Timmer LW, Garnsey SM, Graham JH (eds) Compendium of Citrus Diseases, 2nd edn. APS Press, St. Paul, p. 71

Carbone I., Kohn L.M. 1999. A method for designing primer sets for speciation studies in filamentous ascomycetes. *Mycologia* 91: 553–556.

Conzulex W., Ramallo J., Ploper L.D. 1997. Identification of *Fusarium solani* (Mart.) associated with decline and root rot of grapefruit (*Citrus paradisi*). *Avana Agroindustrial* 18: 7–8.

Crous P.W., Verkley G.J.M., Groenewald J.Z., Houbraken, J. 2019. *Westerdijk Laboratory Manual Series* 1: Fungal Biodiversity. Westerdijk Fungal Biodiversity Institute, Utrecht, The Netherlands.

Derrick K.S., Timmer L.W. 2000. Citrus Blight and other diseases of recalcitrant etiology. *Annual Review of Phytopathology* 38: 181–205.

El-Mohamedy R.S.R. 1998. Studies on Wilt and Root Rot Disease of Some Citrus Plants in Egypt. PhD thesis, Fac Agric Ain Shams Univ, Cairo, Egypt, 227 pp.

Esparham N., Mohammadi H., Gramaje D. 2020. A survey of trunk disease pathogens within citrus trees in Iran. *Plants* 9: 754.

Fang D.Q., Federici C.T., Roose M.L. 1998. A high-resolution linkage map of the citrus tristeza virus resistance gene region in *Poncirus trifoliata* (L.) Raf. *Genetics* 150: 883–890.

FAOSTAT 2019. Food and Agriculture Organization of the United Nations. http://www.fao.org/faostat/en/#home. Accessed 26 February 2020.

Fisher N.L., Burguess L.W., Toussoun T.A., Nelson P.E. 1982. Carnation leaves as a substrate and for preserving cultures of *Fusarium* species. *Phytopathology* 72: 151–153.

Gräfenhan T., Schroers H.J., Nirenberg H.I., Seifert K.A. 2011. An overview of the taxonomy, phylogeny, and typification of nectriaceous fungi in *Cosmospora*, *Acremonium*, *Fusarium*, *Stilbella*, and *Volutella*. *Studies in Mycology* 68: 79–113.

Graham J.H., Brlansky R.H., Timmer L.W., Lee R.F., Marais, L.J. 1985. Comparison of citrus tree declines with necrosis of major roots and their association with *Fusarium solani*. *Plant Disease* 69: 1055–1058.

Guarnaccia V., Crous P.W. 2018. Species of *Diaporthe* on *Camellia* and *Citrus* in the Azores Islands. *Phytopathologia Mediterranea* 57: 307–319.

Guarnaccia V., Sandoval-Denis M., Aiello D., Polizzi G., Crous, P.W. 2018. *Neocosmospora perseae* sp. nov., causing trunk cankers on avocado in Italy. *Fungal Systematics and Evolution* 1: 131–140.

Guarnaccia V., Aiello D., Polizzi G., Crous, P.W., Sandoval-Denis M. 2019. Soilborne diseases caused by *Fusarium* and *Neocosmospora* spp. on ornamental plants in Italy. *Phytopathologia Mediterranea* 58: 127–137.

Hannachi I., Rezgui S., Cherif M. 2014. First report of mature citrus trees being affected by Fusarium wilt in Tunisia. *Plant Disease* 98: 566.

Huelsenbeck J.P., Ronquist F. 2001. MrBayes: Bayesian inference of phylogeny. *Bioinformatics* 17: 754–755.

Katoh K., Rozewicki J., Yamada K.D. 2019. MAFFT online service: multiple sequence alignment, interactive sequence choice and visualization. *Briefings in Bioinformatics* 20: 1160–1166.

Kore S.S., Mane A.V. 1992. A dry root rot disease of kagzilime (*Citrus aurantifolia*) seedling caused by *Fusarium solani*. *Journal of Maharashtra Agricultural Universities* 17: 276–278.

Kurt Ş., Uysal A., Soylu E., Kara M., Soylu S. 2020. Characterization and pathogenicity of *Fusarium solani* associated with dry root rot of citrus in the eastern Mediterranean region of Turkey. *Journal of General Plant Pathology* 86: 326–332.

Leslie J.F., Summerell B.A. 2006. *The Fusarium laboratory manual*. Blackwell Publishing, Ames.

Liu Y.J., Whelen S., Hall B.D. 1999. Phylogenetic relationships among ascomycetes: evidence from an RNA polymerase II subunit. *Molecular Biology and Evolution* 16: 1799–1808.

Lombard L., Van der Merwe N.A., Groenewald J.Z., Crous P.W. 2015. Generic concepts in Nectriaceae. *Studies in Mycology* 80: 189–245.

Malikoutsaki-Mathioudi M., Bourbos V.A., Skoudridakis M.T. 1987. La pourriture sèche des racines – une maladie très grave des agrumes en Grèce. *EPPO Bulletin* 17: 335–340.

Mason-Gamer R., Kellogg E. 1996. Testing for phylogenetic conflict among molecular data sets in the tribe *Triticeae* (*Gramineae*). Systematic Biology 45: 524–545.

Mayorquin J.S., Nouri M.T., Peacock B.B., Trouillas F.P., Douhan G.W., … Eskalen A. 2019. Identification, Pathogenicity, and Spore Trapping of *Colletotrichum karstii* associated with twig and shoot dieback in California. *Plant Disease* 103: 1464–1473.

Menge J.A. 1988. Dry root rot. In: Whiteside JO, Garnsey SM, Timmer LW (eds), *Compendium of Citrus diseases*, 14–15. APS Press, USA.

Miller M.A., Pfeiffer W., Schwartz T. 2012. The CIPRES science gateway: enabling high-impact science for phylogenetics researchers with limited resources. In: *Proceedings of the 1st Conference of the Extreme Science and Engineering Discovery Environment: Bridging from the extreme to the campus and beyond*, 1–8. Association for Computing Machinery, USA.

Nemec S., Baker R. 1992. Observations on *Fusarium solani* naphthazarin toxins, their action, and potential role in citrus plant disease. *Proceedings of the 7th meeting of the International Society of Citriculture*, Acireale, Italy, International Society of Citriculture, Riverside, pp. 832–837.

Nemec S., Baker R., Burnett H. 1980. Pathogenicity of *Fusarium solani* to citrus roots and its possible role in blight etiology. *Proceedings of the Florida State Horticultural Society* 93: 36–41.

Nirenberg H.I. 1976. Untersuchungen über die morphologische und biologische differenzierung in der Fusarium-Sektion Liseola. *Mitteilungen der Biologischen Bundesanstalt für Land- und Forstwirtschaft Berlin-Dahlem* 169: 1–117.

Nylander J.A.A. 2004. MrModeltest v2. Program distributed by the author. Evolutionary Biology Centre, Uppsala University.

O'Donnell K., Sutton D.A., Fothergill A., McCarthy D., Rinaldi M.G., … Geiser D.M. 2008. Molecular phylogenetic diversity, multilocus haplotype nomenclature, and in vitro antifungal resistance within the *Fusarium solani* species complex. *Journal of Clinical Microbiology* 46: 2477–2490.

O'Donnell K, Sutton DA, Rinaldi MG, Sarver, B. A., Balajee, S. A., … Aoki T. 2010. Internet-accessible DNA sequence database for identifying fusaria from human and animal infections. *Journal of Clinical Microbiology* 48: 3708–3718.

Polizzi G., Magnano di San Lio G., Catara A. 1992. Dry root rot of citranges in Italy. *Proceedings of the International Society of Citriculture*. VII International Citrus Congress, Acireale 1992: 890–893.

Quaedvlieg W., Binder M., Groenewald J.Z., Summerell, B.A., Carnegie, A.J., … Crous P.W. 2014. Introducing the consolidated species concept to resolve species in the Teratosphaeriaceae. *Persoonia* 33: 1–40.

Rayner R.W., 1970. *A Mycological Colour Chart*. Kew, UK: Commonwealth Mycological Institute.

Rehman A., Rehman A., Javed N., Mehboob S. 2012. Toxin production by *Fusarium solani* from declining citrus plants and its management. *African Journal of Biotechnology* 11: 2199–2203.

Ronquist F., Huelsenbeck J.P. 2003. MrBayes 3: Bayesian phylogenetic inference under mixed models. *Bioinformatics* 19: 1572–1574.

Sandoval-Denis M., Crous P.W. 2018. Removing chaos from confusion: assigning names to common human and animal pathogens in *Neocosmospora*. *Persoonia* 41: 109–129.

Sandoval-Denis M., Guarnaccia V., Polizzi G., Crous P.W. 2018. Symptomatic *Citrus* trees reveal a new pathogenic lineage in *Fusarium* and two new *Neocosmospora* species. *Persoonia* 40: 1–25.

Sandoval-Denis M., Lombard L., Crous P.W. 2019. Back to the roots: a reappraisal of *Neocosmospora*. *Persoonia* 43: 90–185.

Smith I.M., Dunez J., Phillips D.H., Lelliott R.A., Archer S.A. 1988. European handbook of plant diseases. Blackwell Scientific Publications, UK.

Spina S, Coco V, Gentile A, Catara A., Cirvilleri G. 2008. Association of *Fusarium solani* with rolabc and wild type Troyer Citrange. *Journal of Plant Pathology* 90: 479–486.

Stamatakis A. 2014. RAxML version 8: a tool for phylogenetic analysis and post-analysis of large phylogenies. *Bioinformatics* 30: 1312–1313.

Sung G.H., Sung J.M., Hywel-Jones N.L., Spatafora J. W. 2007. A multi-gene phylogeny of Clavicipitaceae (Ascomycota, Fungi): Identification of localized incongruence using a combinational bootstrap approach. *Molecular Phylogenetics and Evolution* 44: 1204–1223.

Tamura K., Stecher G., Peterson D., Filipski A., Kumar S. 2013. MEGA6: Molecular Evolutionary Genetics Analysis version 6.0. *Molecular Biology and Evolution* 30: 2725–2729.

Timmer L.W. 1982. Host range and host colonization, temperature effects, and dispersal of *Fusarium oxysporum* f. sp. *citri*. *Phytopathology* 72: 698–702.

Timmer L.W., Garnsey S.M., Grimm G.R., El-Gholl N.E., Schoulties C.L. 1979. Wilt and dieback of Mexican lime caused by *Fusarium oxysporum*. *Phytopathology* 69: 730–734.

Verma K.S., Nartey S., Singh N. 1999. Occurrence and control of dry root rot of citrus seedlings. *Plant Disease Research* 14: 31–34.

Vilgalys R., Hester M. 1990. Rapid genetic identification and mapping of enzymatically amplified ribosomal DNA from several *Cryptococcus* species. *Journal of Bacteriology* 172: 4238–4246.

Vilgalys R., Sun B.L. 1994. Ancient and recent patterns of geographic speciation in the oyster mushroom *Pleurotus* revealed by phylogenetic analysis of ribosomal DNA sequences. *Proceedings of the National Academy of Sciences of the United States of America* 91: 4599–4603.

White T.J., Bruns T., Lee S., Taylor J. 1990. Amplification and direct sequencing of fungal ribosomal RNA genes for phylogenetics. In: Innes MA, Gelfand DH, Sninsky *et al.* (eds), *PCR Protocols: a Guide to Methods and Applications*: 315–322. Academic Press, USA.

Wiens J.J. 1998. Testing phylogenetic methods with tree congruence: phylogenetic analysis of polymorphic morphological characters in phrynosomatid lizards. *Systematic Biology* 47: 427–444.

Yaseen T., D'Onghia A.M. 2012. *Fusarium* spp. associated to citrus dry root rot: An emerging issue for Mediterranean citriculture. *Acta Horticulturae* 940: 647–655.